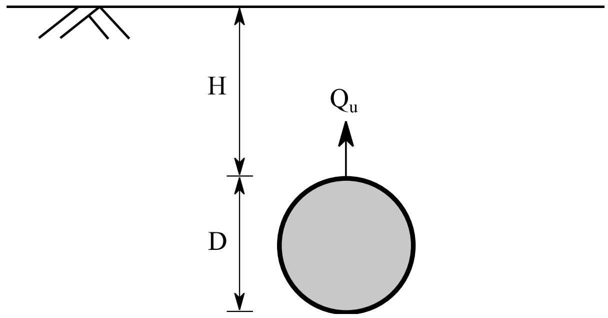

Figure 1. Geometry and notation.

Numerical analysis of the undrained uplift capacity of buried pipelines have generally considered an idealised clay, with uniform or linearly increasing shear strength (e.g. Ballard and Smith 2015; Martin and White 2012). The idealisation of clay as a linear elastic- or rigid-perfectly plastic material may not allow important physical characteristics to be captured. Natural clays often show inter-particle bonding, or structure, which can significantly affect soil response under load (Leroueil and Vaughan 1990) but cannot be simulated by simple elasto-plastic models. Furthermore, spatial variability is an inherent feature of soil deposits both on- and off-shore (e.g. Lacasse and Nadim 1996; Phoon and Kulhawy 1999). Probabilistic studies using random fields to represent spatial variability have shown that the mechanical behaviour and bearing capacity of offshore foundation types such as skirted foundations (Charlton and Rouainia *In press*) and spudcans (Li et al. 2016) in undrained clay can be substantially different from deterministic predictions.

This paper presents finite element analysis of the uplift capacity of a buried pipeline in undrained clay using an advanced critical state constitutive model, formulated within a framework of kinematic hardening, to capture the degradation of clay structure as the pipeline is loaded to its ultimate capacity. The disturbed clay backfill is modelled by a continuum approach, with a random field used to represent the spatial variability of clay structure around the pipeline. Statistics of the uplift capacity are computed by Monte Carlo simulation and a parametric study is undertaken to identify the effect of the coefficient of variation (COV) and autocorrelation length of clay structure on uplift behaviour.

CONSTITUTIVE MODEL

The rate-independent kinematic hardening structure model (KHSM) developed by Rouainia and Muir Wood (2000) is used to describe the effect of clay structure on pipeline uplift capacity. The KHSM extends the conventional Modified Cam Clay (MCC) model by including an initial amount of structure that is progressively destroyed until a fully remoulded state is reached, represented by the reference MCC yield surface. The KHSM introduces a kinematic hardening bubble and an outer structure surface to describe the state and effect of soil structure. The bubble, reference and structure surface have the same elliptical shape.

The essential feature of the KHSM is the degradation of structure in the soil as plastic strain accumulates. The degree of structure is firstly specified by the parameter r_0, which controls the initial size of the structure surface in relation to the reference surface ($r_0 \geq 1$). The degradation of this initial structure is modelled by the following damage law:

$$r = 1 + (r_0 - 1)exp\left[\frac{-k\varepsilon_d}{(\lambda^* - \kappa^*)}\right]$$

where r is the current structure in the soil. The damage law is a monotonically decreasing function of a damage strain, ε_d, and the minimum value of r is 1 when structure and reference surfaces coincide. The parameter k controls the rate of structure degradation, while λ^* and κ^* are respectively the slope of the normal compression line and swelling line in a volumetric strain-logarithmic mean stress plot. Damage strain is calculated from the volumetric (ε_v^p) and shear (ε_q^p) components of plastic strain by a relationship between the strain rates:

$$\dot{\varepsilon}_d = \left[(1-A)\dot{\varepsilon}_v^{p2} + A\dot{\varepsilon}_q^{p2}\right]^{1/2}$$

where A is a dimensionless parameter that determines how ε_v^p and ε_q^p contribute to the damage strain and the degradation of structure in the soil.

NORRKÖPING CLAY

The KHSM parameters are calibrated to triaxial test results from Norrköping clay, an inorganic clay of low sensitivity. The calibration procedure was undertaken and reported by Rouainia and Muir Wood (2000), where further details of the model parameters may be found. The calibrated parameters are given in Table 1. An effective unit weight of $\gamma' = 8\text{kN/m}^3$ is considered throughout and the initial stress conditions are generated by K_0 consolidation, with K_0 equal to 0.4489. The clay is normally consolidated as this is typical of seabed sediments and represents the conditions relevant in the reconsolidated backfill material in a pipeline trench.

Table 1. Calibrated soil parameters for Norrköping clay.

Material property	Value
Slope of swelling line, κ^*	0.0297
Slope of normal compression line, λ^*	0.252
Poisson's ratio, v	0.29
Critical state stress ratio, M	1.35
Ratio of size of bubble and reference surface, R	0.145
Stiffness interpolation parameter, B	1.98
Stiffness interpolation exponent, ψ	1.547
Initial degree of structure, r_0	1.75
Destructuration strain parameter, A	0.494
Destructuration parameter, k	4.16

REPRESENTATION OF SPATIAL VARIABILITY

The spatial variability of clay structure is considered by modelling the KHSM parameter r_0 as a random field. The choice of probability density function (PDF) and autocorrelation structure of r_0 is not straightforward as there is limited information available in the literature about the statistics of clay structure. For the analysis of the undrained capacity of a buried pipeline the effect of clay structure can be understood by its influence on the undrained shear strength, s_u. Figure 3 shows the results of simulated undrained triaxial compression tests on isotropically consolidated samples of Norrköping clay. The effect of increasing r_0 is to increase the peak value of s_u. The sensitivity of the clay is also greater, as r_0 does not affect the size of the MCC yield surface and so the remoulded s_u, simulated by setting r_0 = 1, remains the same. The monotonic relationship between r_0 and s_u indicates that basing the statistics of r_0 on those of the undrained shear strength is a reasonable choice.

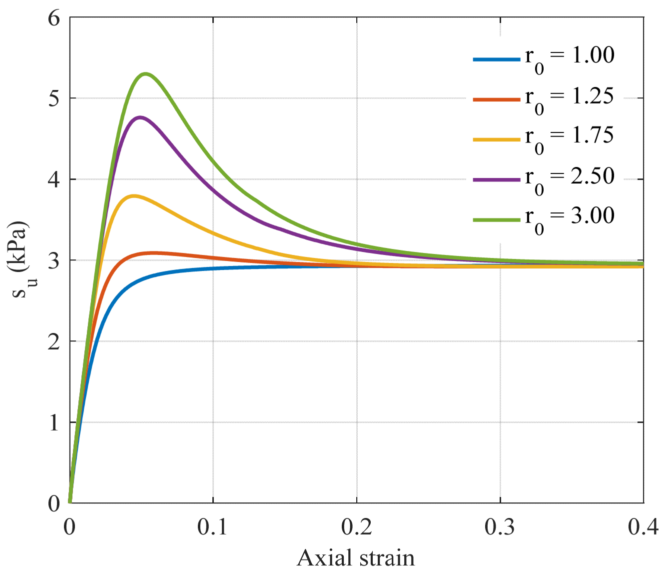

Figure 2. Effect of r_0 on the s_u-axial strain response in simulated undrained triaxial tests on Norrköping clay.

Lacasse and Nadim (1996) found that a lognormal distribution is appropriate for modelling s_u and Ching and Phoon (2012) also observed that several properties of structured clays, including peak and remoulded s_u, could be satisfactorily represented by a lognormal distribution. However, the minimum value for r_0 is 1 so a shifted lognormal distribution is considered here: $r_0 \sim ln\,\mathcal{N}(\alpha, \beta^2, \delta)$. The cumulative distribution function (CDF), F, of the shifted lognormal distribution is:

$$F(r_0; \alpha, \beta, \delta) = \Phi\left(\frac{ln(r_0 - \delta) - \alpha}{\beta}\right)$$

where Φ is the Gaussian CDF with zero mean and unit variance. The first two distribution fitting parameters, α and β, are respectively the mean and standard deviation of the natural logarithm of r_0. A third parameter δ is introduced in order to move the lower bound of the distribution; δ is taken to be 1 so that r_0 cannot take values inadmissible in the KHSM.

The calibrated value of r_0 is considered to be the mean value (μ_{r_0}= 1.75). This reflects the fact that the spatial variability of structure is inherent to the intact clay as well as the backfilled material. Keaveny et al. (1989) found that the autocorrelation, ρ, of s_u can be represented by either an exponential or square exponential function. In this study, a square exponential function is chosen with autocorrelation distances θ_x and θ_y in horizontal (x) and vertical (y) directions respectively.

The shifted lognormal random field of r_0 can be generated as follows:

$$r_0(x, y) = \delta + \exp(\alpha + \beta G(x, y))$$

where $G(x, y)$ is a correlated Gaussian random field of zero mean and unit variance and is discretised on a rectangular grid using the expansion optimal linear estimation (EOLE) method (Li and Der Kiureghian 1993). The shifted lognormal distribution is strongly non-Gaussian and the mapping from a Gaussian to non-Gaussian marginal distribution distorts the autocorrelation structure, particularly when the COV is high. Fortunately, the autocorrelation in the underlying Gaussian space can be found analytically in this case (Liu and Der Kiureghian 1986). The correlation distortion is such that the autocorrelation matrix of $G(x, y)$, $\mathbf{\Sigma}^G$, was not positive-semi definite in all analysis cases considered in this paper. This can introduce serious errors into the correlation and marginal distribution of the non-Gaussian random field, so a strategy of computing the nearest correlation matrix to the analytically-computed $\boldsymbol{\Sigma}^G$ was implemented, similar to that proposed in Kim and Shields (2015). This method ensures that $r_0(x, y)$ has the prescribed autocorrelation.

FINITE ELEMENT MODEL

A plane strain finite element model (Plaxis 2012) is used to compute the uplift capacity pipeline of diameter D = 0.25m buried at a depth H = 0.875m. The dimensionless embedment ratio H/D = 3.5. This is chosen as being representative of a typical pipeline diameter and embedment. The finite element mesh is shown in Figure 6 and consists of 539 15-noded triangular elements, with the mesh refined in the region around the pipeline. Here, the pipe is assumed to have a rough surface, as might be the case if a concrete coating was applied, and the pipe and soil are attached with an infinite tensile capacity. The random field is generated on a fine stochastic mesh, separate from the finite element mesh, and values of r_0 are mapped to the finite element Gauss points using linear shape functions.

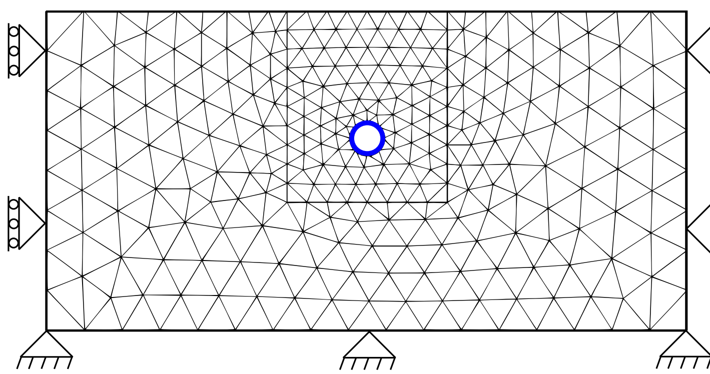

Figure 3. Finite element mesh.

DETERMINISTIC ANALYSIS

Figure 4(a) shows the load-displacement curves for a uniform r_0. For structured clay (r_0 = 1.75), a peak force is reached before softening occurs as plastic strains develop and structure is degraded. In contrast, in remoulded clay (r_0 = 1) the load continues to increase until an ultimate value is reached. This ultimate force is equal to that of the structured clay at large displacements due to complete remoulding of the clay along the failure planes.

The failure mechanisms are shown in Figure 4(b) and in both cases a deep, flow-around mechanism forms. An exact solution has been derived for this mechanism, with $N_c = Q_u / Ds_u$ = 11.94 (Randolph and Houlsby 1984). Table 2 gives the capacity factors for both structured and remoulded clay. The reference undrained shear strength, $s_{u,ref}$, is taken at the centre of the pipe and calculated by simulating a plane strain compression test using the in-situ stress conditions. A good match is observed in the remoulded clay, with the value of N_c overestimated by less than 3%. In structured clay, the capacity factor is predicted to be 25% less than the exact value. However, the plasticity solution does not take into account degradation of structure, which reduces the capacity factor due to a progressive failure as plastic strains develop.

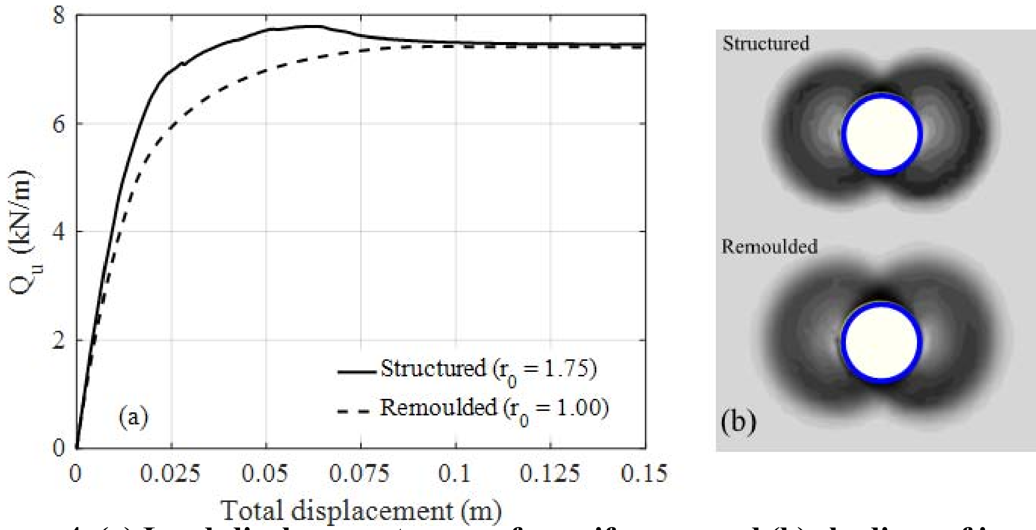

Figure 4. (a) Load-displacement curves for uniform r_0 and (b) shadings of incremental displacements at 0.15m displacement.

Table 2. Capacity factors in structured and remoulded clay.

Case	$s_{u,ref}$(kPa)	Q_u (kN/m)	N_c
Structured (r_0 = 1.75)	3.52	7.79	8.85
Remoulded (r_0 = 1.00)	2.42	7.42	12.26

EFFECT OF COV

A parametric study was undertaken with COV_{r0} = {0.1, 0.3, 0.5} to cover the typical range of variability of s_u (Phoon and Kulhawy 1999). For these analyses, θ_x and θ_y are fixed at 1.5m (6D) and 0.25m (1D) respectively. Load-displacement plots from 500 simulations are presented in Figure 5 for COV_{r0} = 0.1 and 0.5. Figure 5(a) shows that when COV_{r0} is low, the load-displacement responses are very similar to the deterministic analysis with a uniform $r_0 = \mu_{r_0}$= 1.75. In each case a peak load is reached before softening occurs and the load reduces to the remoulded value. It can be inferred that a flow-around mechanism governs the response.

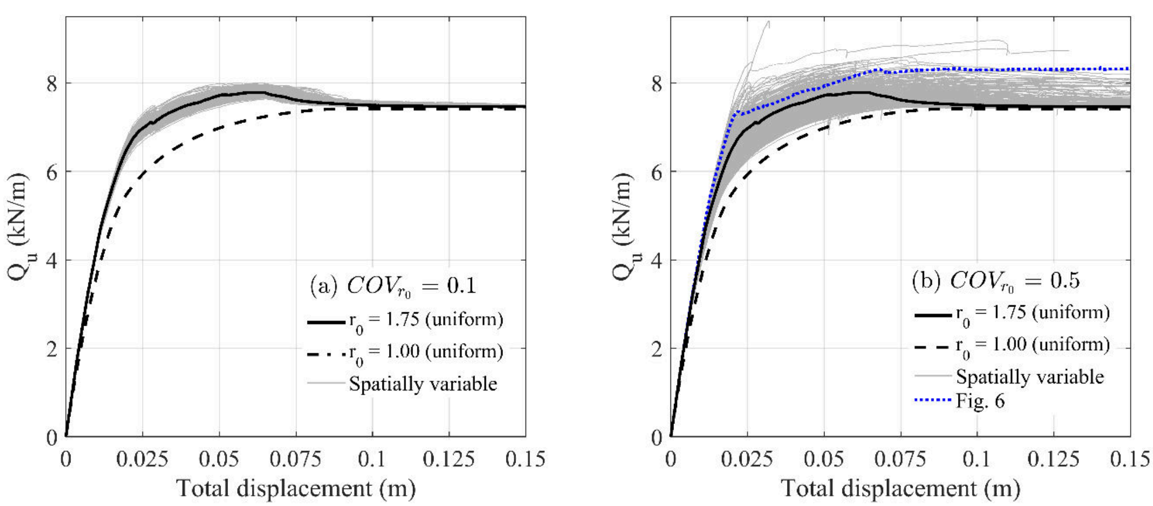

Figure 5. Load-displacement curves for 500 simulations with (a) COV_{r0} = 0.1 and (b) COV_{r0} = 0.5.

In contrast, as evident in Figure 5(b) when COV_{r0} = 0.5 there is a much wider range of load-displacement responses. Importantly, the spatial distribution of clay structure can be seen to influence the type of failure. Figure 6 shows the failure mechanism from a simulation with COV_{r0} = 0.5; the corresponding load-displacement response is indicated in Figure 5(b). For this case, a reverse bearing capacity mechanism forms involving a block of soil being lifted upwards with the pipe rather than the flow-around mechanism that occurs when r_0 is uniform or the spatial distribution has a low variability (e.g. COV_{r0} = 0.1). Instead of post-peak softening behaviour, the load-displacement curve shows an increase to a constant ultimate load that, for this specific simulation, is higher than the peak force observed with r_0 = 1.75.

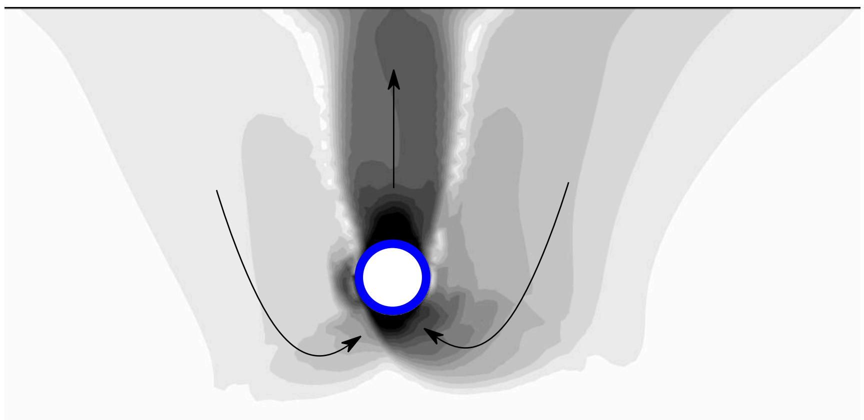

Figure 6. Failure mechanism from a simulation with COV_{r0} = 0.5.

The effect of COV_{r0} on the mean ultimate load (μ_{Qu}) is shown in Figure 7(a). Confidence intervals are computed by 10,000 bootstrap samples. When the variability of r_0 is low, μ_{Qu} is close to the deterministic analysis with a uniform r0. Further investigation is required to determine whether the higher μ_{Qu} at COV_{r0} = 0.1 relative to the uniform capacity is a result of a physical mechanism or model non-linearity, or can be attributed to statistical error. The effect of increasing COV_{r0} is to reduce μ_{Qu}; while there are cases of very high peak loads when COV_{r0} = 0.5, as discussed previously, they must occur fairly infrequently and the flow-around failure is the predominant mechanism. The extreme peak loads contribute to the increase in the COV of the ultimate load with COV_{r0}, as shown in Figure 7(b).

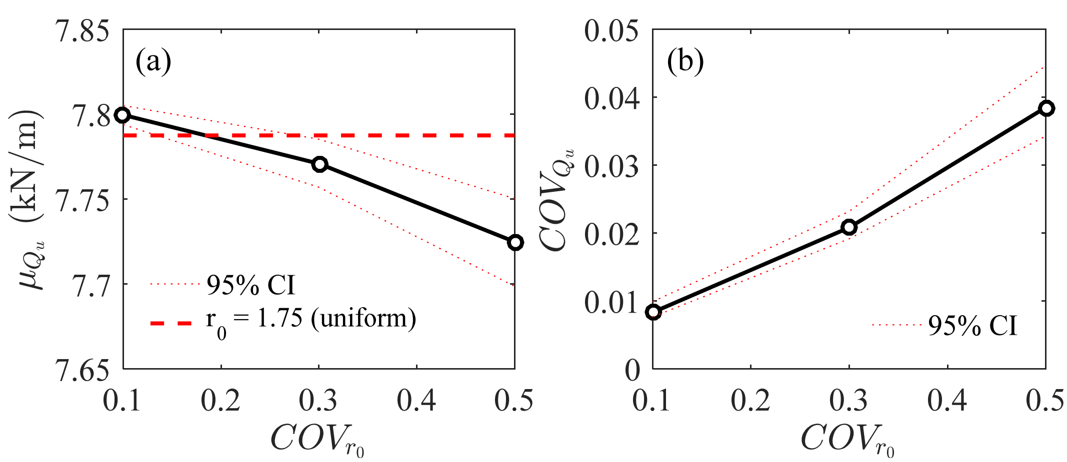

Figure 7. Effect of COV_{r0} on (a) Mean ultimate load, μ_{Qu}, and (b) COV of ultimate load, COV_{Qu}.

EFFECT OF AUTOCORRELATION DISTANCE

A further parametric study was carried out to identify the effect of autocorrelation distance on pipeline uplift capacity. Correlation of soil parameters is generally anisotropic, with correlation in the horizontal distance often an order of magnitude greater than in the vertical direction (Lacasse and Nadim 1996). The parameter ranges investigated in this study are θ_x = {0.25m (1D), 0.75m (3D), 1.5m (6D), 2.5m (10D)} and θ_y = {0.125m (0.5D), 0.25m (1D), 0.5m (2D), 1m (4D)}. The horizontal autocorrelation distance is chosen to be similar to the width of a typical, steep-sided pipeline trench (DNV 2007). The default autocorrelation distances are θ_x = 6D and θ_y = D, while COV_{r0} = 0.3. For all cases, 500 simulations were run to characterise the response.

The autocorrelation distance has less influence on μ_{Qu} than COV_{r0}, but important effects were observed on the load-displacement behaviour. Figure 8 presents the load-displacement curves for the extreme values of θ_x and θ_y. From Figure 8(a) and (b) it can be seen that the increase in θ_x from 1D to 10D leads to a greater spread in the load-displacement curves from the end of the elastic range to a total displacement of 0.15m (0.6D). The tendency of some curves to reach a plateau or show only limited softening behaviour is indicative of a reverse bearing capacity mechanism. As evident in Figure 8(c), these curves are present when the vertical correlation is short but for θ_y = 4D, shown in Figure 8(d), the load-displacement behaviour shows a peak and subsequent softening with nearly all cases reducing to the remoulded capacity at large displacements.

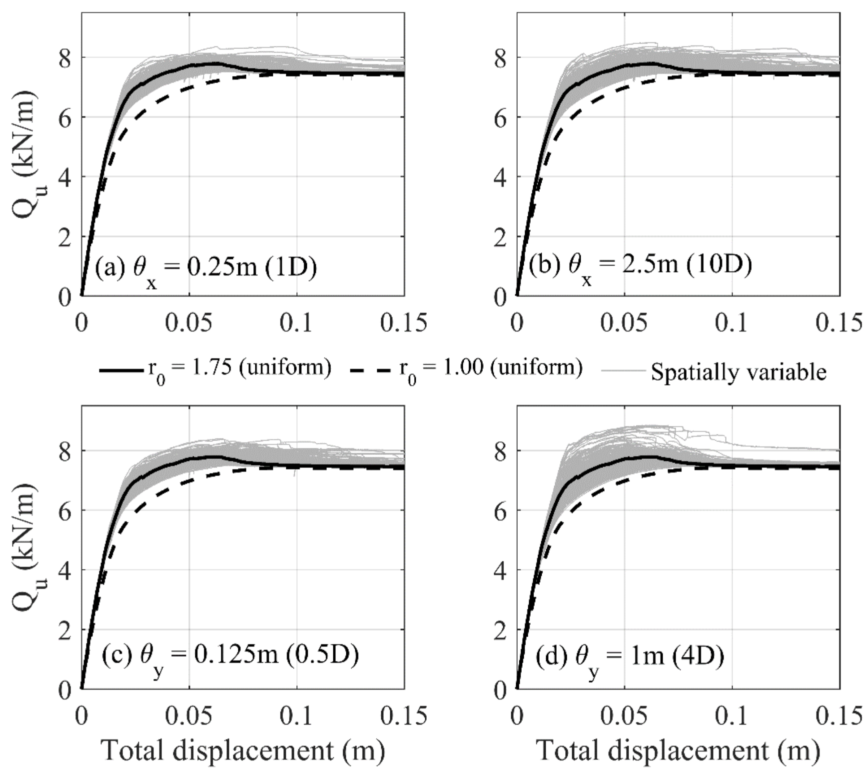

Figure 8. Load-displacement curves for (a) θ_x = 0.25m (1D), (b) θ_x = 2.5m (10D), (c) θ_y = 0.125m (0.5D) and (d) θ_y = 1m (4D).

The effect of the autocorrelation distance on the failure characteristics of the pipeline can be further assessed by considering the displacement at which the peak load occurs, denoted d_{peak}. In Figure 9(a), the mean of d_{peak} ($\mu_{d,peak}$) is shown as θ_x is increased from 1D to 10D. With a longer autocorrelation distance in the x-direction, $\mu_{d,peak}$ also increases suggesting that the reverse bearing capacity mechanism becomes more frequent. On the other hand, Figure 9(b) shows that when θ_y increases, $\mu_{d,peak}$ is reduced, particularly when the vertical autocorrelation length is similar to the pipeline diameter. This reflects the load-displacement behaviour observed in Figure 8 and suggests that the flow-around failure becomes the principal mechanism. This conclusion is strengthened by the fact that, as shown in Figure 9(d), the COV of d_{peak} decreases with longer θ_y, implying that the response is increasingly governed by one type of failure mechanism. In contrast, Figure 9(c) shows that a longer θ_x results in higher $COV_{d,peak}$, suggesting a range of possible failure modes involving flow-around of the clay or lifting of a block of soil with the pipe.

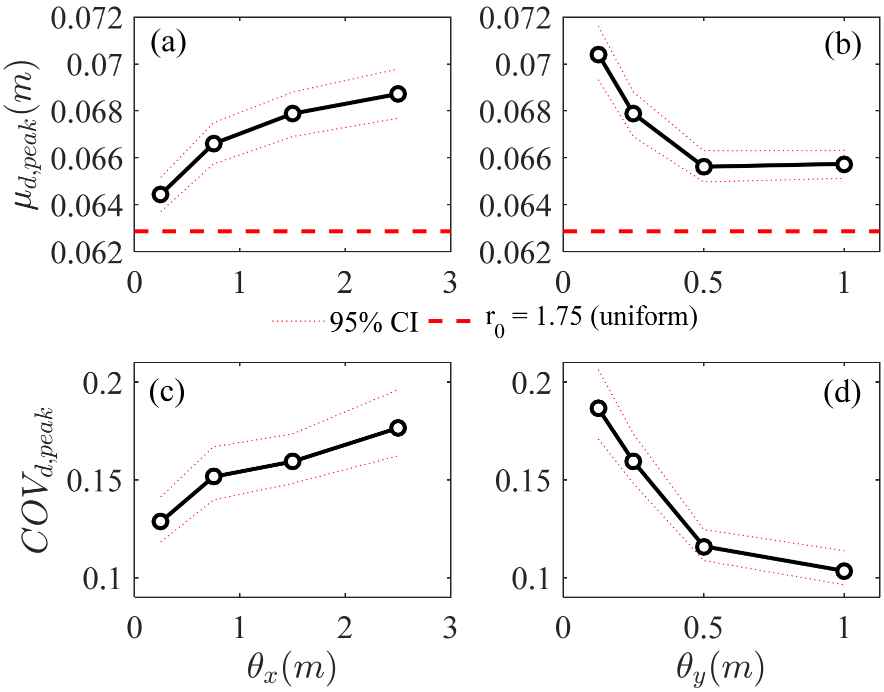

Figure 9. Effect of autocorrelation length on (a)-(b) mean displacement at peak load, $\mu_{d,peak}$, and (c)-(d) COV of the displacement at peak load, $COV_{d,peak}$.

CONCLUSION

A study of pipeline uplift capacity in an undrained clay with spatially variable structure has been conducted. The effect of clay structure on mechanical behaviour was described using the KHSM, an advanced kinematic hardening constitutive model. The model has been implemented in a finite element code and coupled with a random field representation of the parameter r_0, which describes the initial degree of structure. In a deterministic analysis with a uniform spatial distribution of r_0, a flow-around failure mechanism formed and the load-displacement curve showed a peak load before softening. The failure mechanism was unaffected if the spatial variability of r_0 is low but for higher COV_{r0} failure could be influenced by the lifting of a block of soil with the pipe. With increasing COV_{r0}, the mean of the ultimate load reduced but the variability increased as a result of the different mechanisms occurring. Longer vertical autocorrelation favoured the formation of a flow-around mechanism. The study demonstrates that the spatial variability of clay structure has an important effect on the uplift behaviour of a pipeline.

ACKNOWLEDGEMENTS

The first author is supported by a studentship grant from the Engineering and Physical Sciences Research Council (EPSRC) and Atkins. This support is gratefully received and acknowledged.

REFERENCES

Ballard, J.-C., and Smith, C. C. (2015). "Ultimate uplift capacity of buried pipelines in undrained clay." *International Symposium on Frontiers in Offshore Geotechnics III (ISFOG)*, Taylor & Francis, Oslo, Norway.

Charlton, T. S., and Rouainia, M. (in press). "A probabilistic approach to the ultimate capacity of skirted foundations in spatially variable clay." *Struct. Saf*.

Ching, J., and Phoon, K.-K. (2012). "Modeling parameters of structured clays as a multivariate normal distribution." *Can. Geotech. J.*, 49(5), 522-545.

DNV (2007). "DNV-RP-F110 Global buckling of submarine pipelines: Structural design due to high temperature/high pressure." Det Norske Veritas (DNV), Oslo, Norway.

Keaveny, J. M., Nadim, F., and Lacasse, S. (1989). "Autocorrelation Functions for Offshore Geotechnical Data." *5th ICOSSAR*, San Francisco, USA.

Kim, H., and Shields, M. D. (2015). "Modeling strongly non-Gaussian non-stationary stochastic processes using the Iterative Translation Approximation Method and Karhunen–Loève expansion." *Comput. Struct.*, 161, 31-42.

Lacasse, S., and Nadim, F. (1996). "Uncertainties in Characterising Soil Properties." *Uncertainty in the Geologic Environment*, New York: ASCE, 49-75.

Leroueil, S., and Vaughan, P. R. (1990). "The general and congruent effects of structure in natural soils and weak rocks." *Géotechnique*, 40(3), 467-488.

Li, C., and Der Kiureghian, A. (1993). "Optimal Discretization of Random Fields." *J. Eng. Mech.*, 119(6), 1136-1154.

Li, J. H., et al. (2016). "Random finite element method for spudcan foundations in spatially variable soils." *Eng. Geol.*, 205, 146-155.

Liu, P.-L., and Der Kiureghian, A. (1986). "Multivariate distribution models with prescribed marginals and covariances." *Probab. Eng. Mech.*, 1(2), 105-112.

Maconochie, A., Kennedy, J., and Oliphant, J. (2015). "An integrated approach to pipeline burial in the 21st century - The current state-of-the-art." *International Symposium on Frontiers in Offshore Geotechnics III (ISFOG)*, Taylor & Francis, Oslo, Norway.

Martin, C. M., and White, D. J. (2012). "Limit analysis of the undrained bearing capacity of offshore pipelines." *Géotechnique*, 62(9), 847-863.

Palmer, A. C., Ellinas, C. P., Richards, D. M., and Guijt, J. (1990). "Design of pipelines against upheaval buckling." *Offshore Technology Conference* Houston, TX, 551-560.

Phoon, K. K., and Kulhawy, F. H. (1999). "Characterization of geotechnical variability." *Can. Geotech. J.*, 36(4), 612-624.

Plaxis (2012). "PLAXIS 2D 2012 - Reference Manual.", Delft.

Randolph, M., and Houlsby, G. T. (1984). "The limiting pressure on a circular pile loaded laterally in cohesive soil." *Géotechnique*, 34(4), 613-623.

Randolph, M. F., and Gourvenec, S. (2011). *Offshore geotechnical engineering*, Spon Press.

Rouainia, M., and Muir Wood, D. (2000). "A kinematic hardening constitutive model for natural clays with loss of structure." *Géotechnique*, 50(2), 153-164.

White, D. J., and Cathie, D. N. (2011). "Geotechnics for subsea pipelines." *International Symposium on Frontiers in Offshore Geotechnics II (ISFOG),* Perth, Australia.

Effect of Spatial Variability on the Earth Pressure of a Rigid Retaining Wall

V. B. Chauhan, S.M.ASCE[1]; S. M. Dasaka, M.ASCE[2]; and U. S. Dasgupta[3]

[1]Ph. D. Student, Dept. of Civil Engineering, Indian Institute of Technology Bombay, Mumbai 400076, India. E-mail: chuahan.vinaybhushan@gmail.com
[2]Associate Professor, Dept. of Civil Engineering, Indian Institute of Technology Bombay, Mumbai 400076, India. E-mail: dasaka@civil.iitb.ac.in
[3]PG Student, Dept. of Civil, Architectural and Environmental Engineering, Univ. of Texas at Austin, TX 78712. E-mail: udasgupta93@gmail.com

Abstract

Present study investigates the influence of spatial variability of soil properties on the lateral thrust on a rigid retaining wall in active condition. Friction angle of the soil is modelled as a lognormal anisotropic random field in two dimensions, using the Cholesky decomposition technique to study the effect of horizontal and vertical scale of fluctuation on the lateral thrust. The Monte Carlo simulation approach is used in association with FLAC^{3D} to highlight the worst-case spatial variability configuration. The study revealed that deterministic analysis employing mean friction angle underestimates the lateral thrust on the wall, as compared to that obtained using a spatially variable soil. For satisfactory performance of a wall, a scaling factor of around 1.5 is required to be used, if lateral active thrust obtained from deterministic analysis is employed in the design calculations. It is concluded from the reliability analysis that between the two practically possible scenarios, high horizontal and vertical scales of fluctuation scenario exhibit higher lateral thrust.

INTRODUCTION

Retaining walls are an essential part of almost all infrastructure projects, to support vertical or near vertical backfills. As the sectional dimensions of retaining wall are the function of lateral thrust on wall, so a precise estimation of thrust on wall is crucial step for deciding the sectional dimensions of retaining wall. Calculation of thrust on retaining wall has usually been done using Coulomb's or Rankine's theories of lateral earth pressures. These theories involve homogeneity of the soil as a primary assumption, which is not the case in actual field. In practice, characteristic value of the soil parameters are estimated by averaging the soil parameters of collected soil sample from few locations. A true estimate of the soil parameters, depends on the sample size, larger the size sample data, better is the estimate but collection of large size sample data involves ample amount of cost and time. To get the large amount of virtual sample data, random field modeling plays a good role without involving much cost and time. This well established method becomes helpful for geotechnical engineers due to its straightforwardness. These virtual data obtained from random field modeling, take into account many configurations of soil variability which might exist in the field. It assists geotechnical engineers to design the foundations of a structure for the worst possible soil configuration. Random field modeling serves as